Supporting information

1. ^{1}H NMR spectra of TFBP

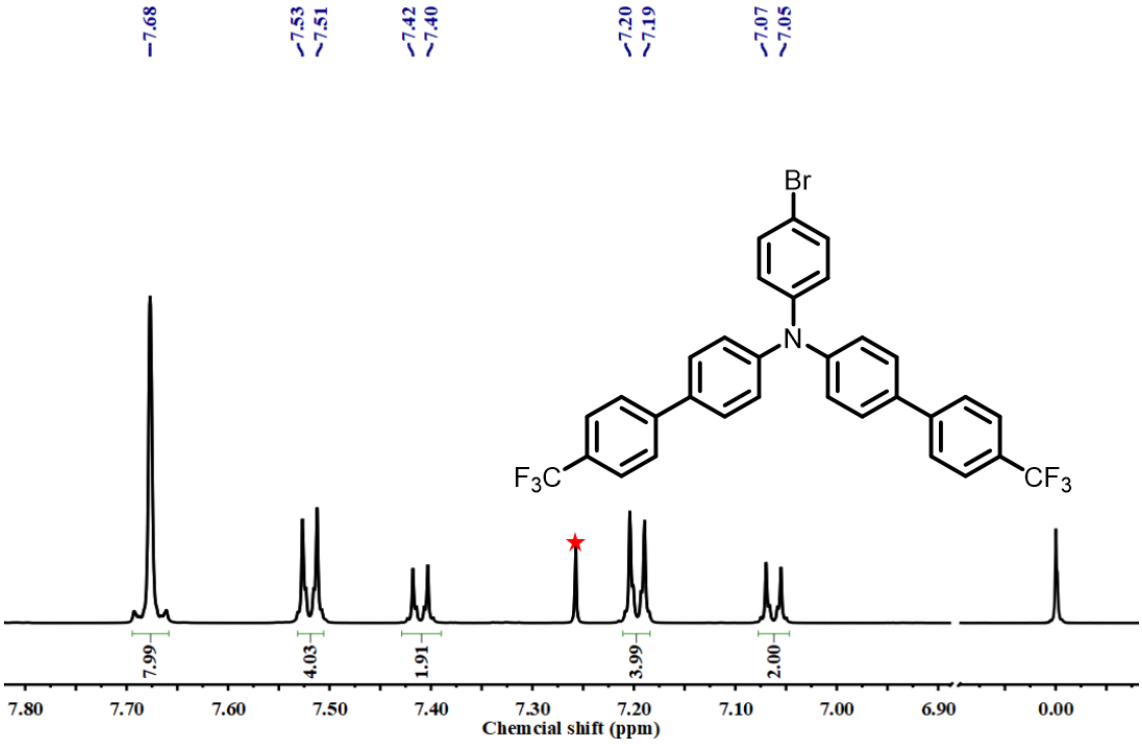

Fig. S1 ^{1}H NMR spectra of TFBP in $CDCl_3$ at room temperature.

2. ^{13}C NMR spectra of TFBP

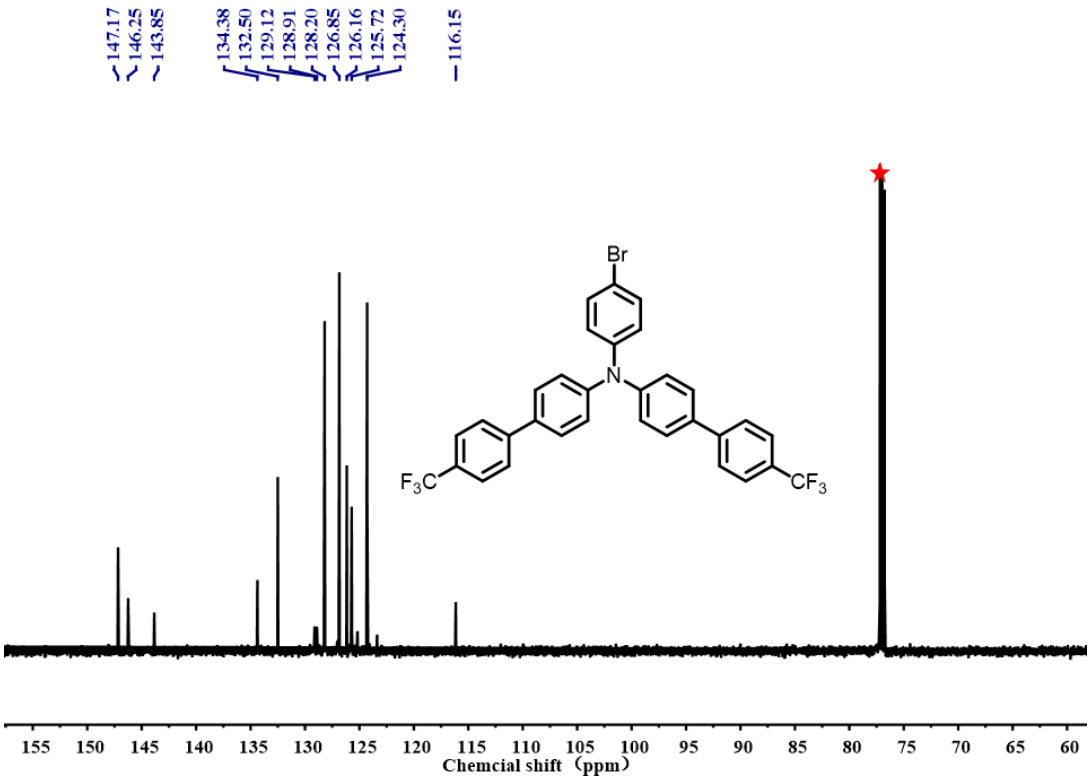

Fig. S2 ^{13}C NMR spectra of TFBP in $CDCl_3$ at room temperature.

3. ^{1}H NMR spectra of TFBP-VB

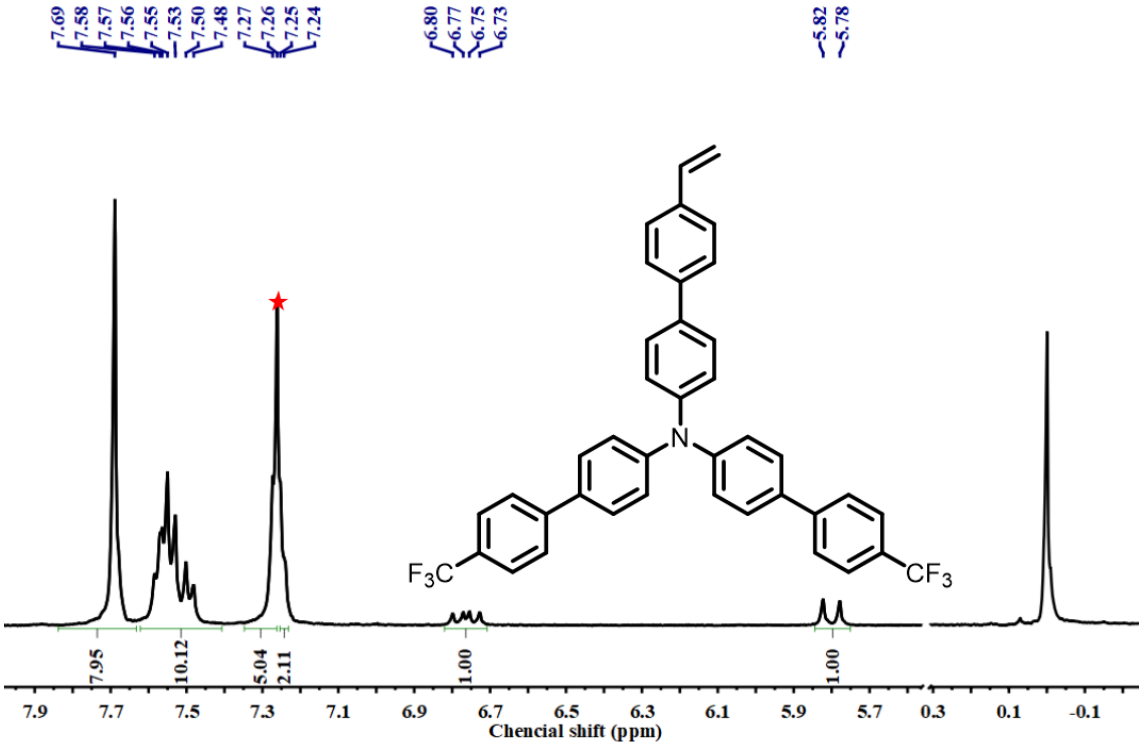

Fig. S3 ^{1}H NMR spectra of TFBP-VB in $CDCl_3$ at room temperature.

4. ^{13}C NMR spectra of TFBP-VB

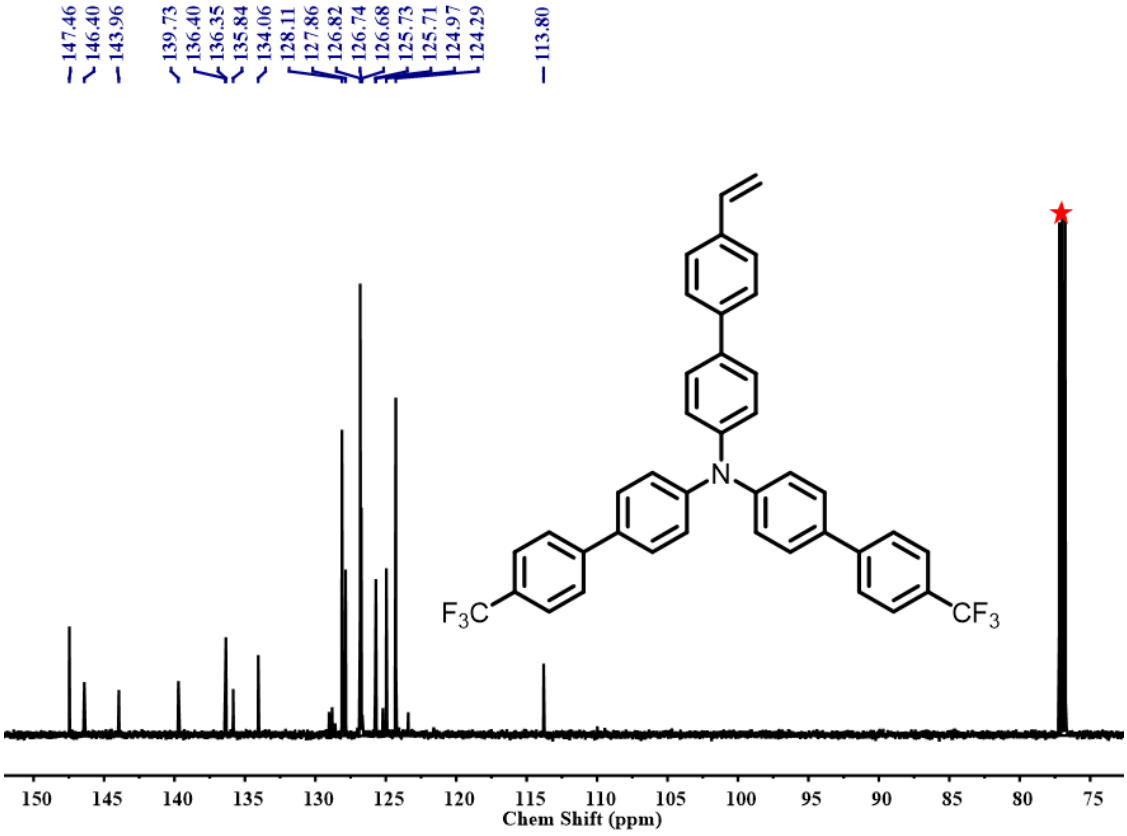

Fig. S4 ^{13}C NMR spectra of TFBP-VB in $CDCl_3$ at room temperature.

5. ^{1}H NMR spectra of TPA-Py

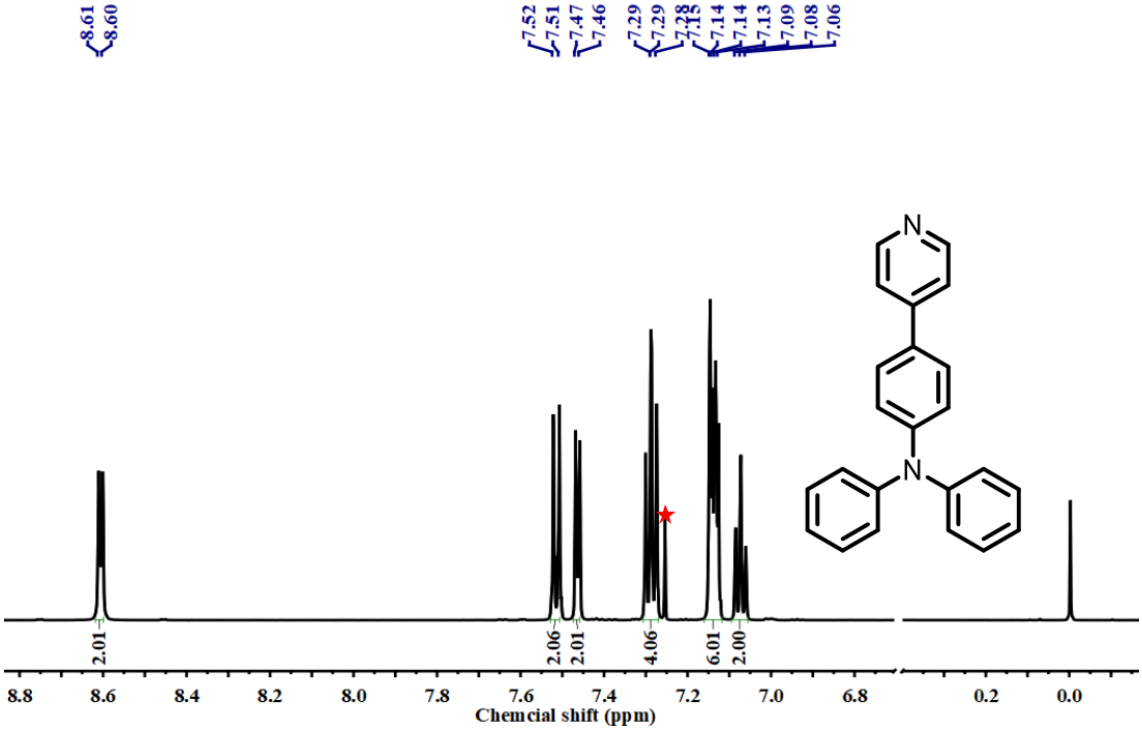

Fig. S5 ^{1}H NMR spectra of TPA-Py in $CDCl_3$ at room temperature.

6. ^{13}C NMR spectra of TPA-Py

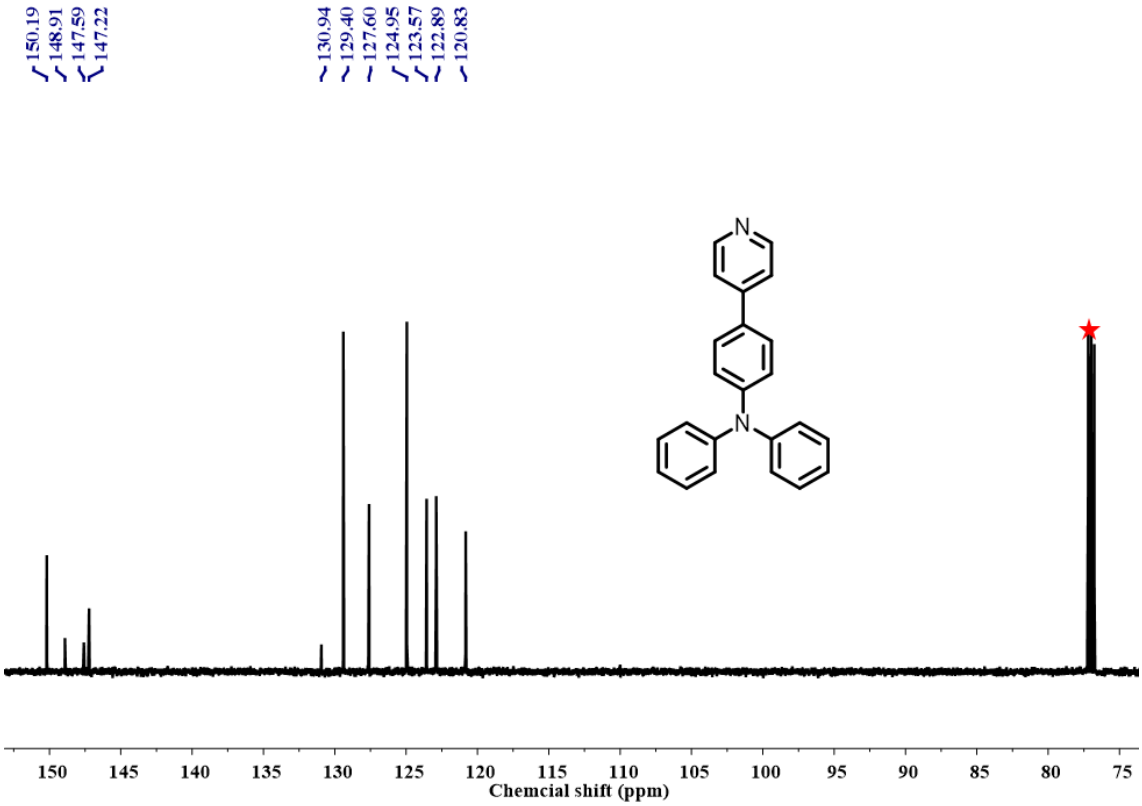

Fig. S6 ^{13}C NMR spectra of TPA-Py in $CDCl_3$ at room temperature.

7. ^{1}H NMR spectra of TPA-Py-CVB

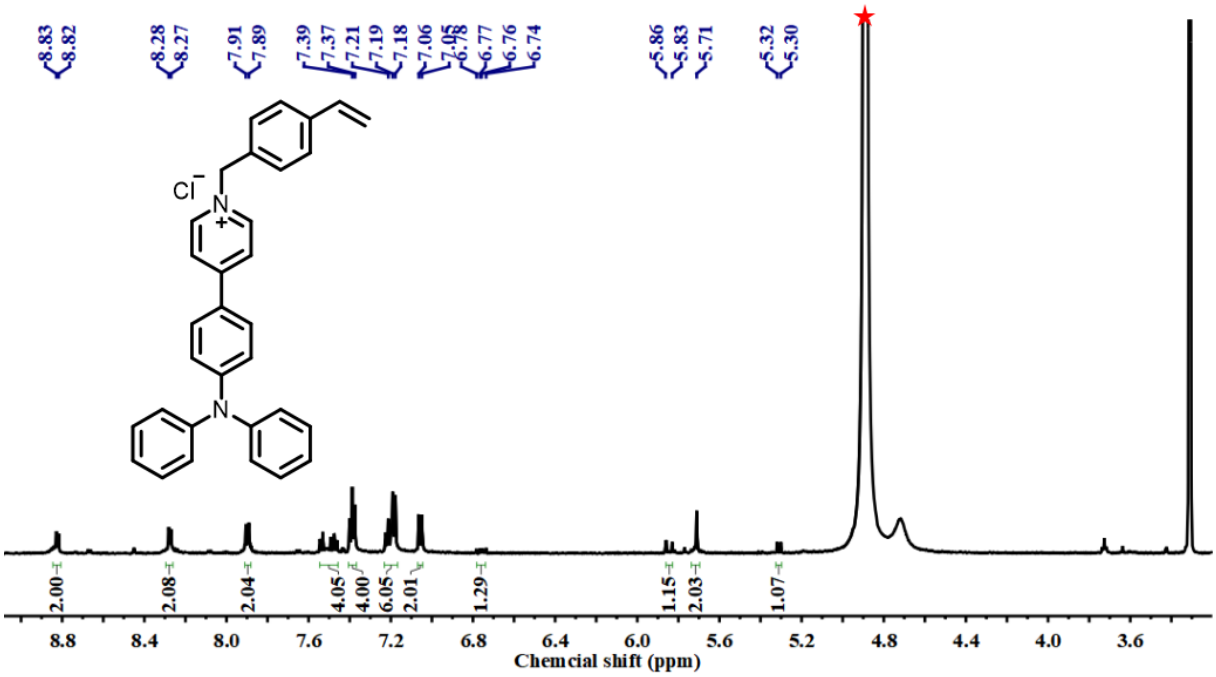

Fig. S7 ^{1}H NMR spectra of TPA-Py-CVB in CD_3OD at room temperature.

8. ^{13}C NMR spectra of TPA-Py-CVB

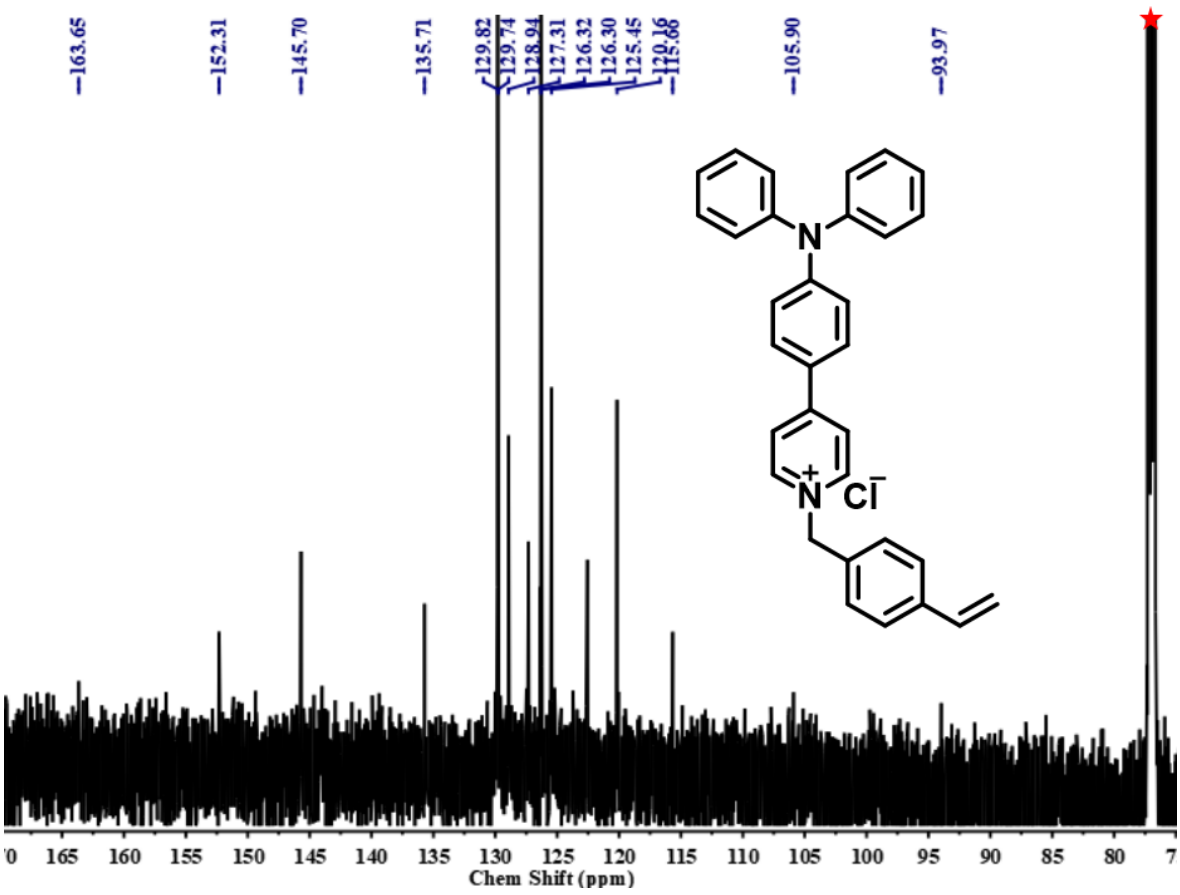

Fig. S8 ^{13}C NMR spectra of TPA-Py-CVB in CD_3Cl at room temperature.

9. ^{1}H NMR spectra of TPA-VPy

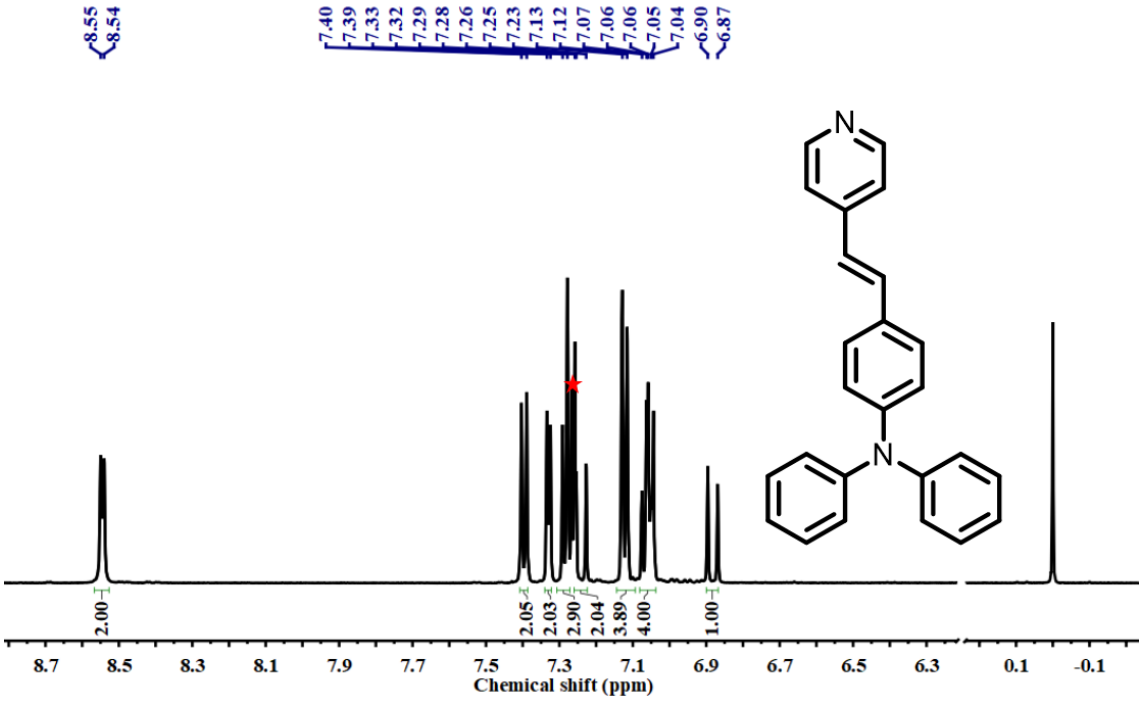

Fig. S9 ^{1}H NMR spectra of TPA-VPy in $CDCl_3$ at room temperature.

10. ^{13}C NMR spectra of TPA-VPy

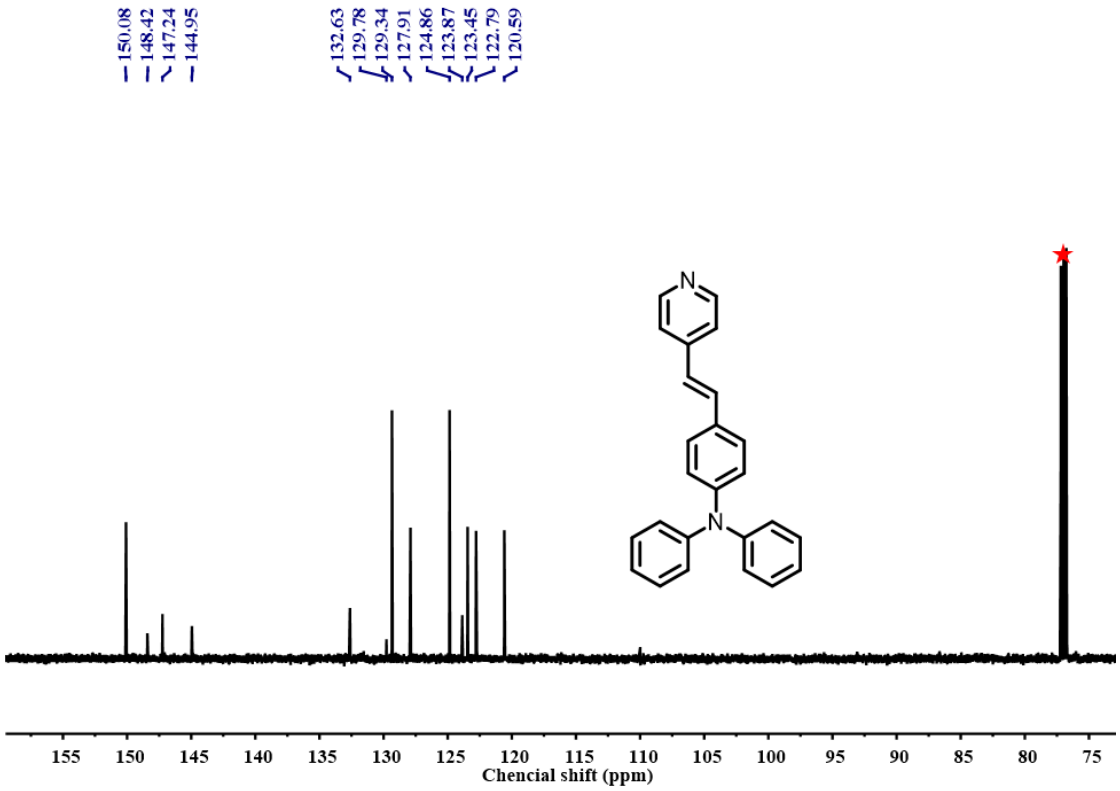

Fig. S10 ^{13}C NMR spectra of TPA-VPy in $CDCl_3$ at room temperature.

11. ^{1}H NMR spectra of TPA-VPy-CVB

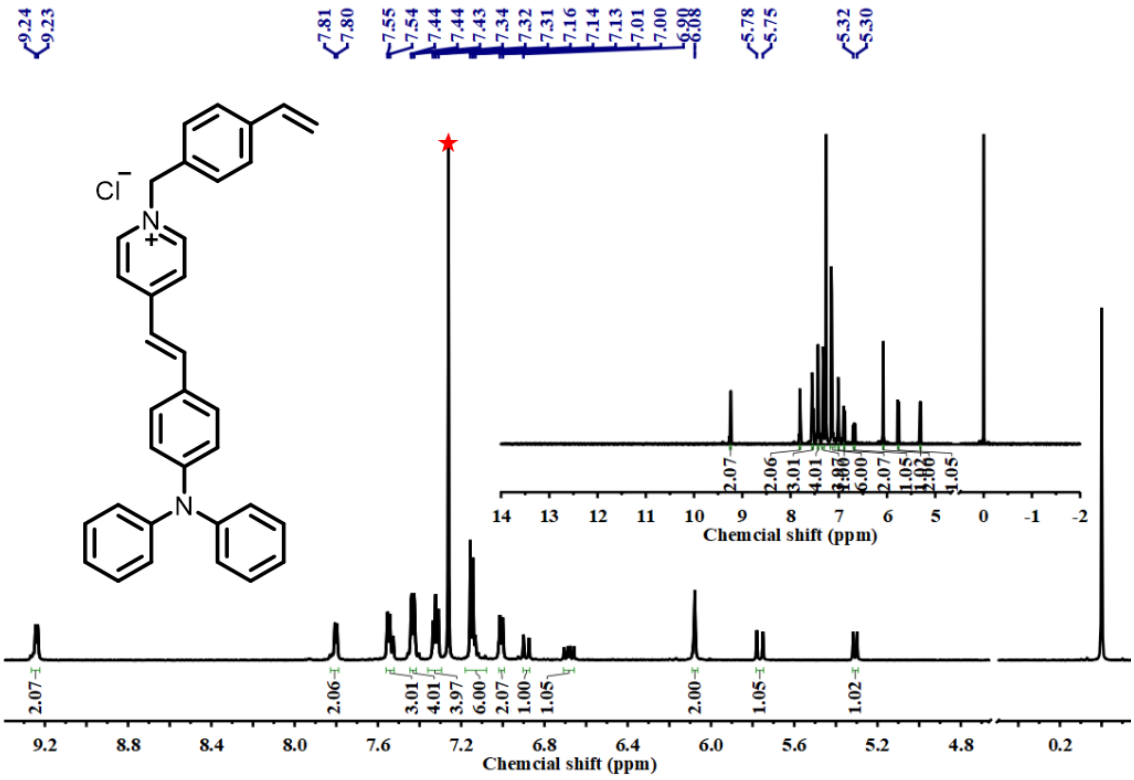

Fig. S11 ^{1}H NMR spectra of TPA-VPy-CVB in $CDCl_3$ at room temperature.

12. ^{1}H NMR spectra of TPA-VPy-CVB

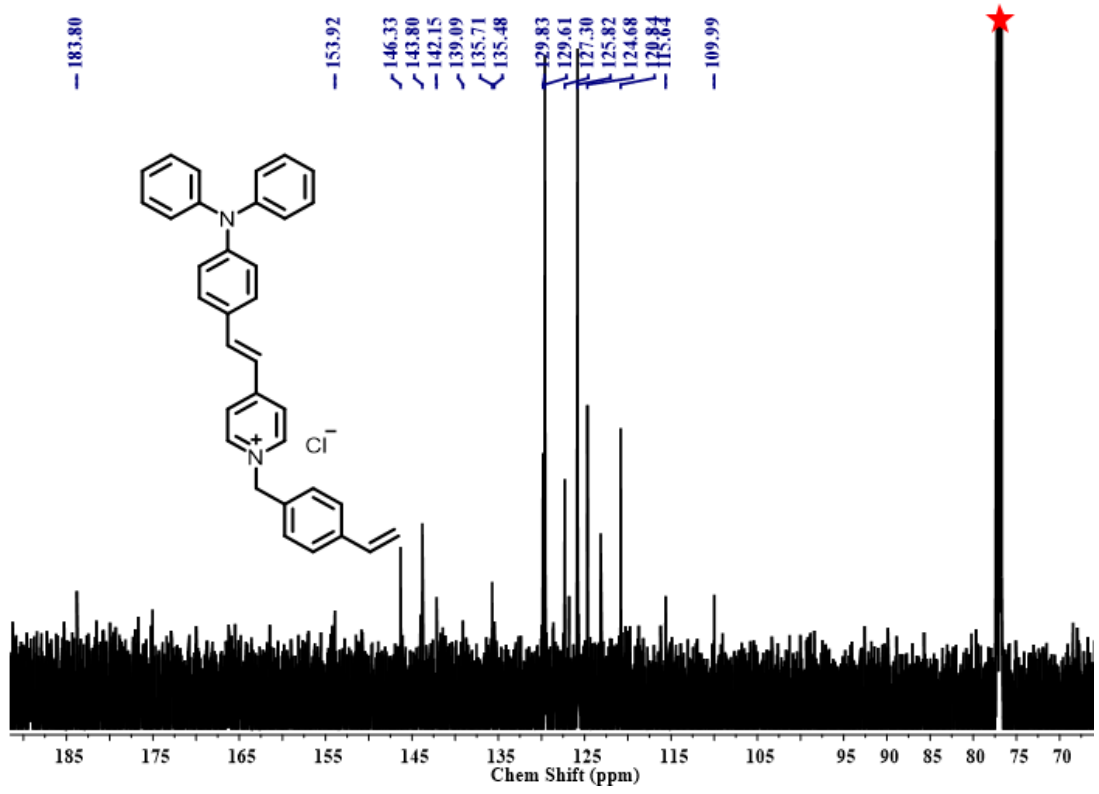

Fig. S12 ^{13}C NMR spectra of TPA-VPy-CVB in $CDCl_3$ at room temperature.

13. Optimized molecular orbital amplitude plots of the HOMO and LUMO energy levels of TPA-Py-CVB, TPA-VPy-CVB.[1]

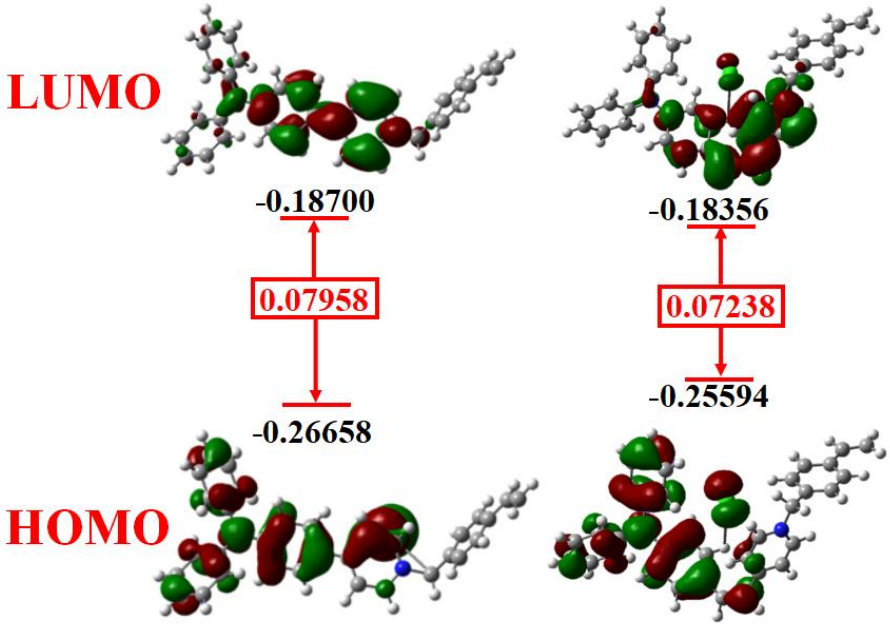

Fig. S13 Optimized molecular orbital amplitude plots of the HOMO and LUMO energy levels of TPA-Py-CVB, TPA-VPy-CVB.

14. Synthetic Routes of P-Orange&Blue

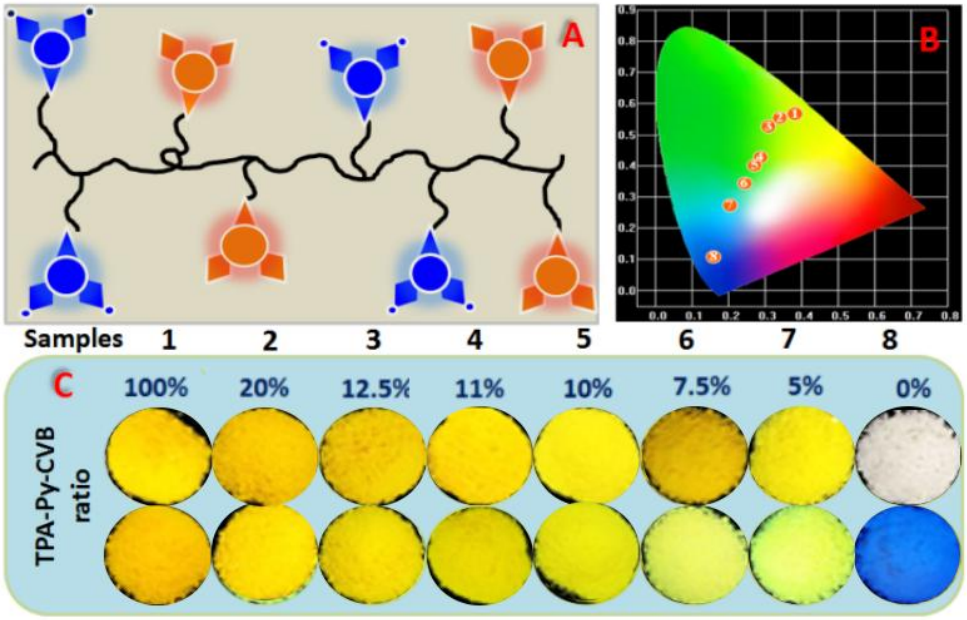

Fig. S14 (a)Synthetic Routes of P-Orange&Blue, The CIE Chromaticity Diagram(c) and photographs(b) of P-Orange&Blue in solid state.

[1] Theoretical calculations using the OPT/FREQ/B3LYP/6-31G* level in the Gaussian 09 program were carried out to characterize the three-dimensional structures and the frontier molecular orbital energy levels of TPA-Py-CVB, TPA-VPy-CVB.

15. The theoretical molar ratios of the fluorophores in the polymers

Table S1 The molar ratios of the fluorophores in the polymers

Polymers	molar ratios of the fluorophores (Blue/Orange)	Polymers	molar ratios of the fluorophores (Blue/Red)
P-Orange	1	P-Red	1
P-Orange&Blue-2	3:1	P-Red&Blue-2	2:1
P-Orange&Blue-3	7:1	P-Red&Blue-3	2.5:1
P-Orange&Blue-4	8:1	P-Red&Blue-4	3:1
P-Orange&Blue-5	9:1	P-Red&Blue-5	4:1
P-Orange&Blue-6	12:1	P-Red&Blue-6	5:1
P-Orange&Blue-7	19:1	P-Red&Blue-7	6:1
P-Blue	1	P-Blue	1

16. ^{1}H NMR spectra of polymers

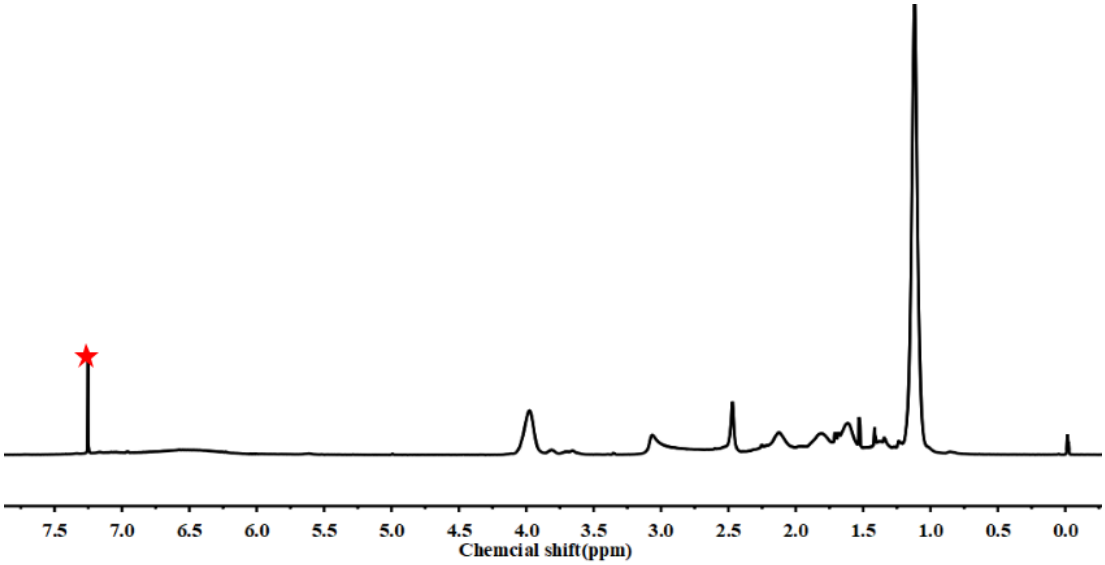

Fig. S15 ^{1}H NMR spectra of P-Orange in $CDCl_3$ at room temperature.

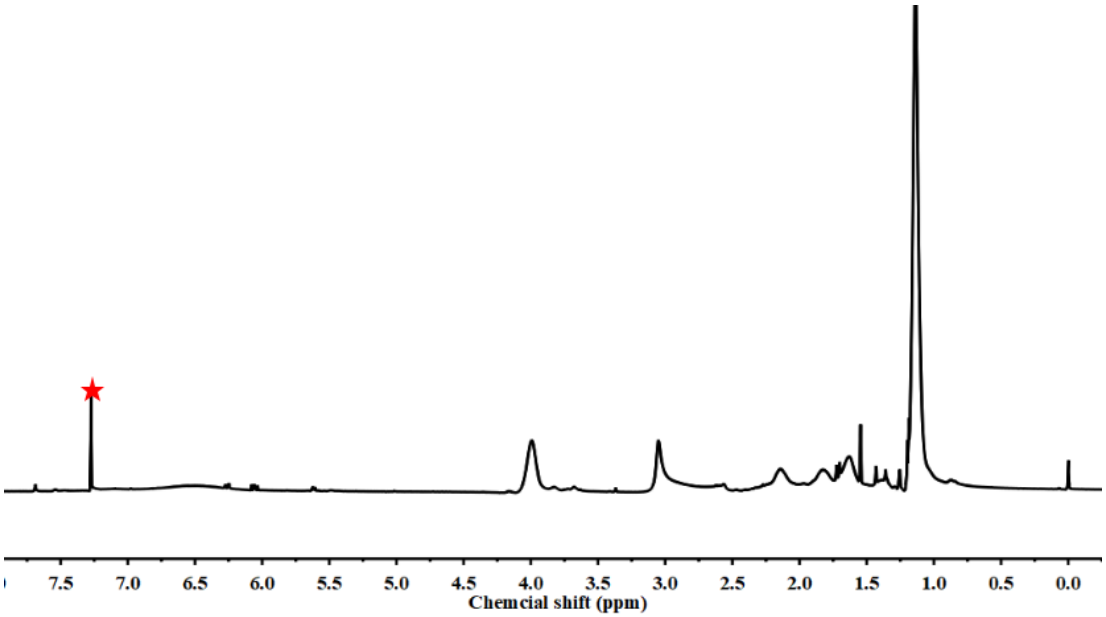

Fig. S16 ^{1}H NMR spectra of P-Blue in $CDCl_3$ at room temperature.

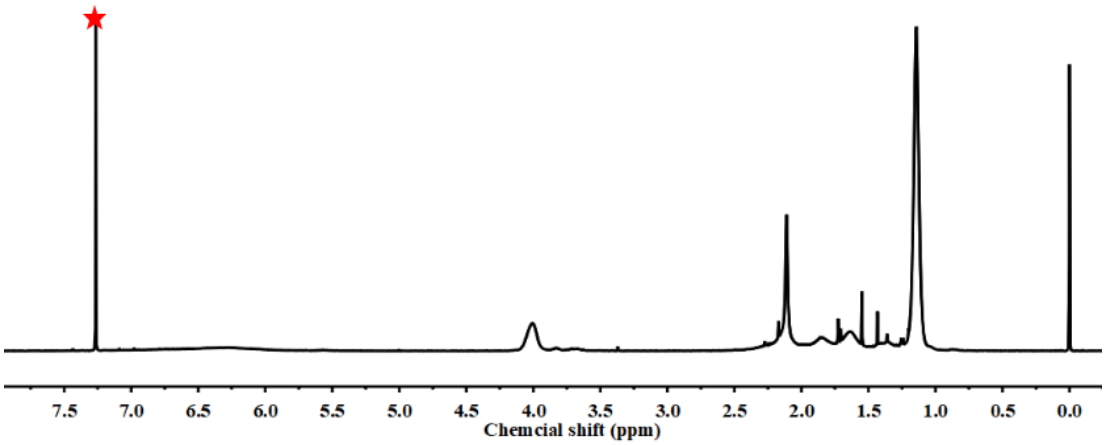

Fig. S17 ^{1}H NMR spectra of P-Orange&Blue-3 in $CDCl_3$ at room temperature.

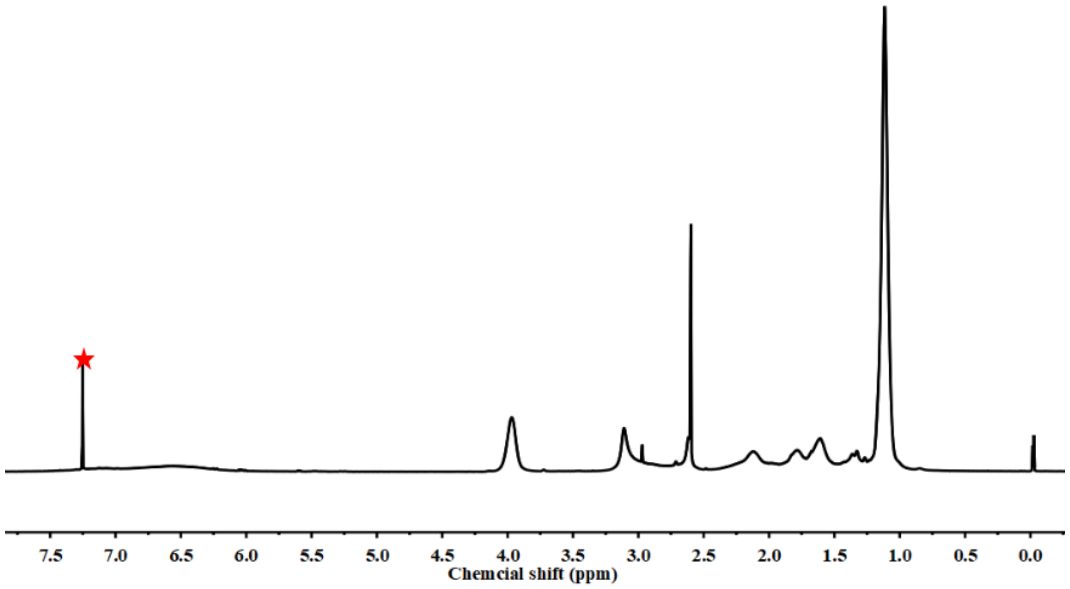

Fig. S18 ^{1}H NMR spectra of P-Red in $CDCl_3$ at room temperature.

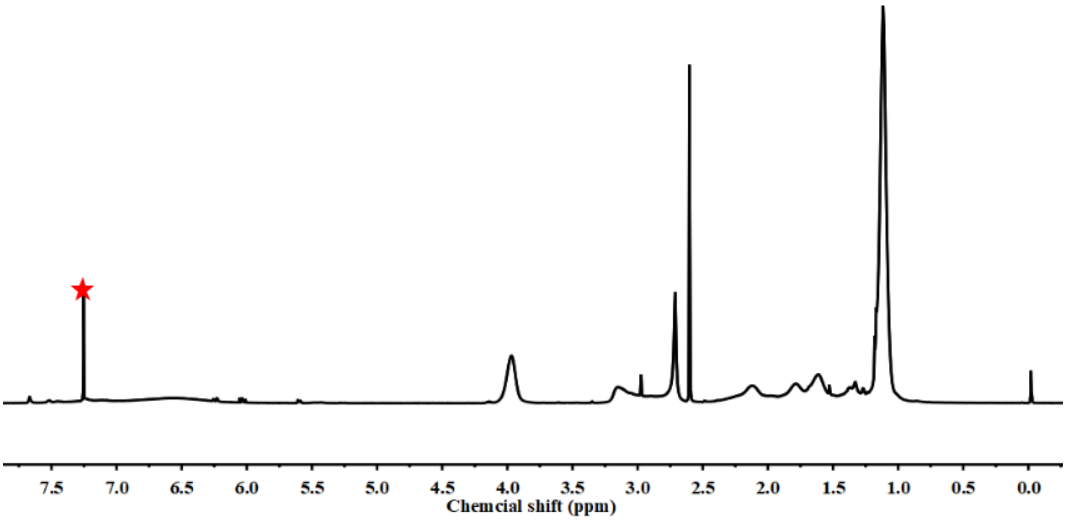

Fig. S19 ^{1}H NMR spectra of P-Red&Blue-3 in $CDCl_3$ at room temperature.

17. Histogram of the integral area of fluorescence spectrum

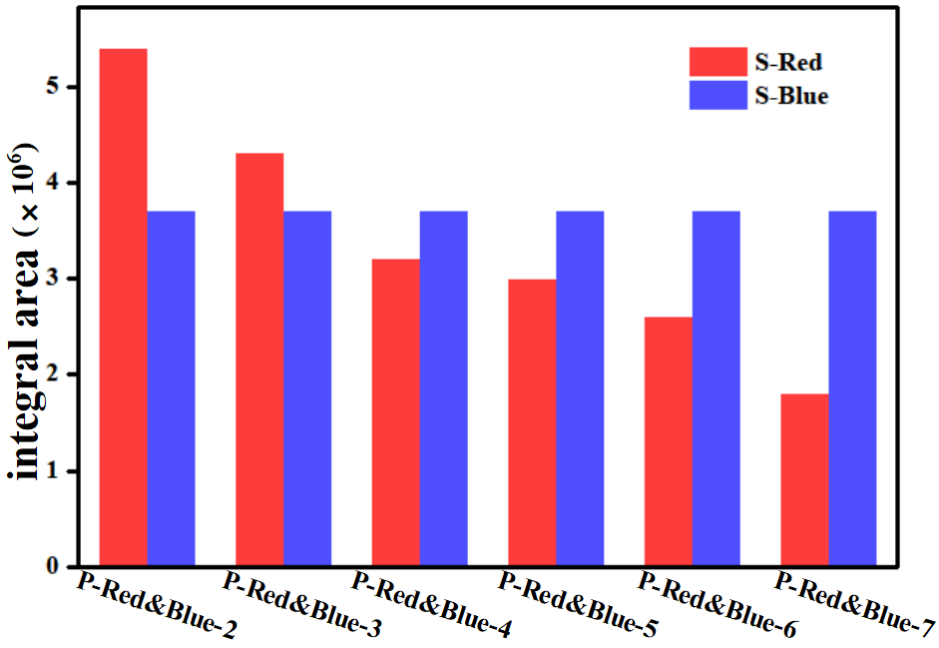

Fig. S20 Histogram of the integral area of fluorescence spectrum of P-Red&Blue2-7.

18. FTIR spectrum of compounds and polymers

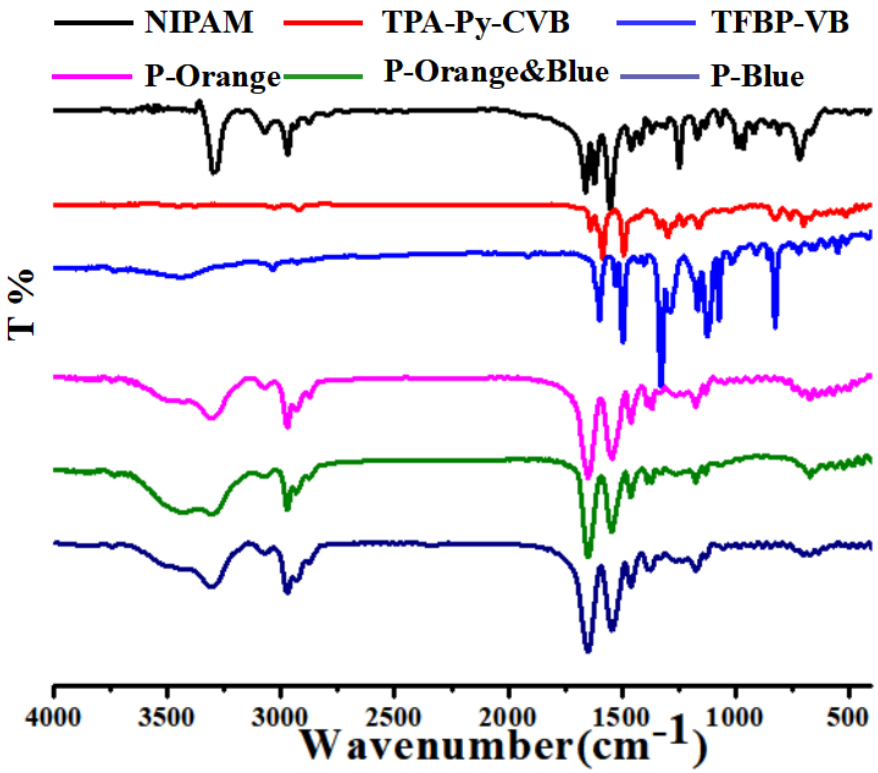

Fig. S21 FTIR spectrum[2] of NIPAM, TPA-Py-CVB, TFBP-VB, P-Orange, P-Orange&Blue-3, P-Blue.

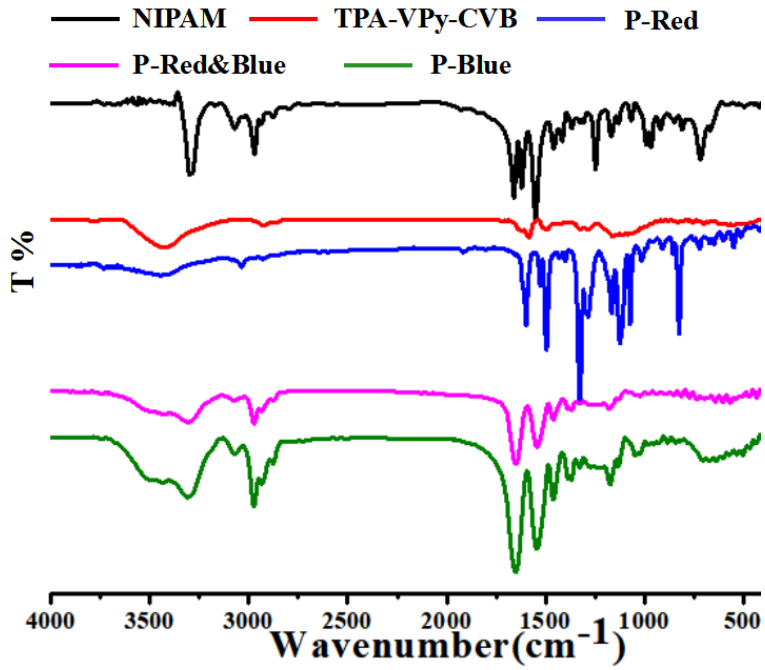

Fig. S22 FTIR spectrum of NIPAM, TPA-VPy-CVB, TFBP-VB, P-Red, P-Blue.

[2] Fourier transform infrared (FT-IR) spectra were recorded on a DIGIL FTS3000 spectrophotometer using KBr tablets.

19. The GPC, LCST , Time-resolved fluorescence and Particle Size data of polymers

Table 1. The GPC[3], LCST[4], Time-resolved fluorescence[5] and Particle Size[6] data of polymers

Polymer	Mn	Mw/Mn	LCST	τ	Particle size
P-Orange	1.104×10^5	3.141	32 ℃	4.81 ns	343 nm
P-Red	1.939×10^3	1.567	34 ℃	3.42 ns	1200 nm
P-Blue	1.515×10^4	1.422	38 ℃	1.75 ns	250 nm
P-Orange&Blue-3	5.794×10^5	1.154	31 ℃	5.31 ns	1060 nm
P-Red&Blue-3	8.296×10^5	1.368	33 ℃	3.99 ns	309 nm

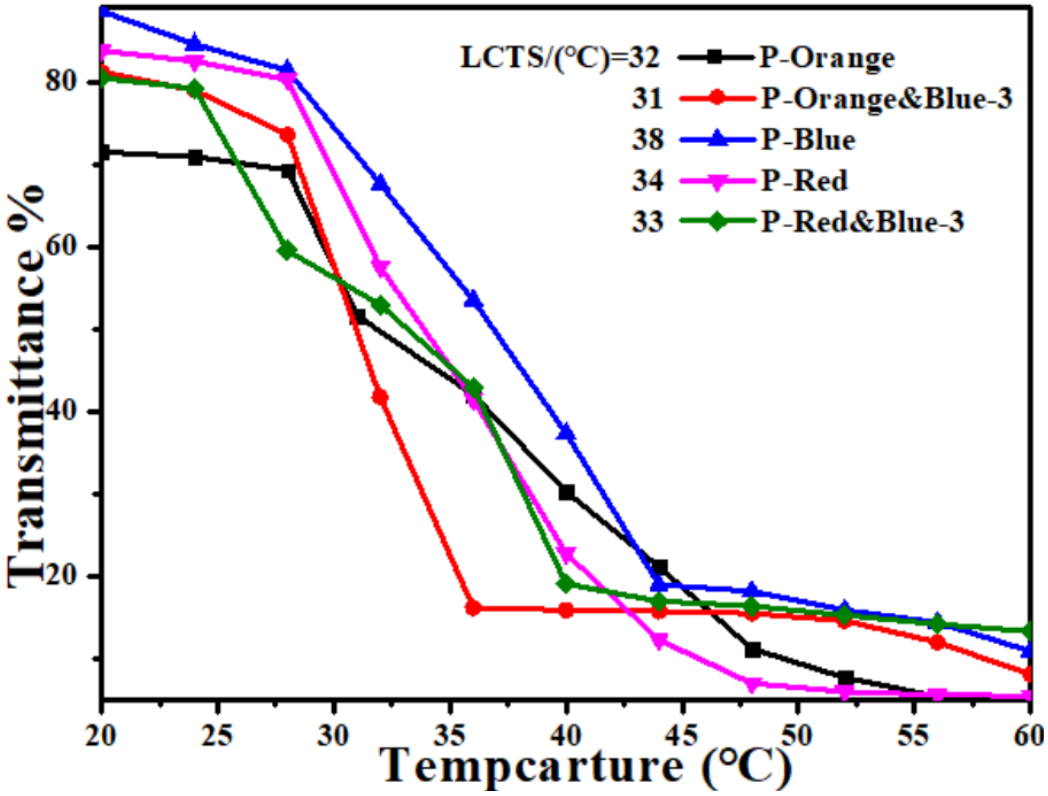

Fig. S23 Tansmittance temperature for polymers in aqueous solution.

[3] The number- and weight-averaged molecular weights (Mn, Mw) were determined by gel permeation chr omatography (GPC).

[4] Turbidity measurements were performed on Z-2000 spectrophotometer equipped in quartz cuvettes of 10 mm path length at a wavelength of 500 nm. In all cases, a polymer concentration of 0.1 mg/mL was employed. Heating rates were 1 °C/min for all measurements. For all clear solutions, the baseline was corrected to zero absorbance, A. Transmittance, $T = 10^{-A}$, was plotted against temperature, and cloud points were determined at 50% transmittance. The maximum temperature was setted as 60 °C for all solutions.

[5] Time-resolved fluorescence measurements were carried out using a C11367-11 Quantaurus-Tau system. The time resolution was 20 ps. The laser energy level for excitation is 2 mW. Decay of the fluorescence intensity (I) with time (t) was fitted by a double-exponential function as shown in Equation (1):

$$\mathbf{I = A_1 e^{-t/\tau_1} + A_2 e^{-t/\tau_2}} \quad (1)$$

in which t_1 and t_2 are the lifetimes of the shorter- and longer-lived species, respectively, and A_1 and A_2 are their respective amplitudes. The weighed mean lifetime (<τ>) was calculated according to Equation (2):

$$< \tau >= \frac{\mathbf{A_1\tau_1+A_2\tau_2}}{\mathbf{A_1+A_2}} \quad (2)$$

[6] Particle size measurements process were performed on a Zetasizer Nano ZS dynamic light scattering (DLS) system. This system determined the particle size distribution of particles in solution, with measurement capability from 0.3 nm to 10 μm. All the samples were tested in aqueous solution.

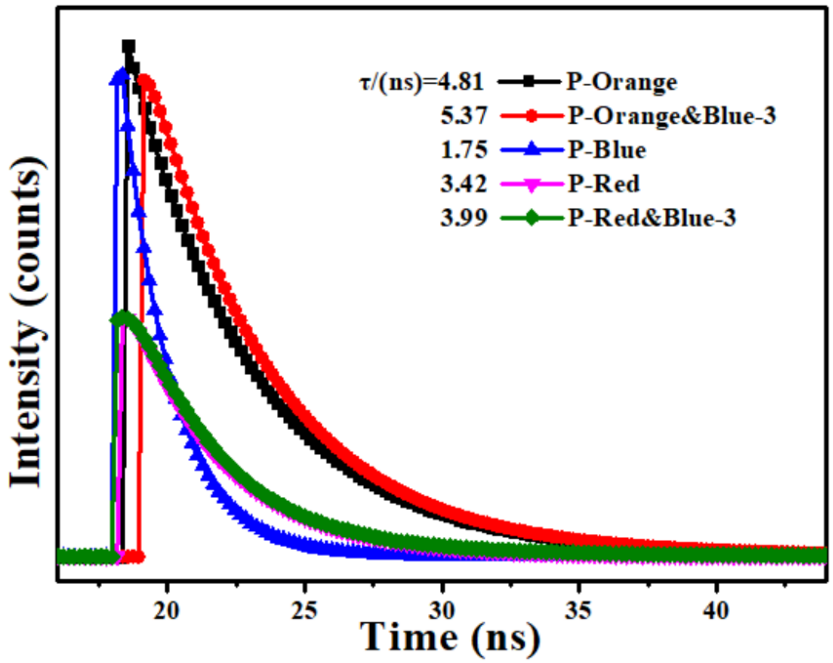

Fig. S24 Time-resolved fluorescence decays of P-Orange, P-Orange-Blue, P-Blue, P-Red, P-Red&Blue.

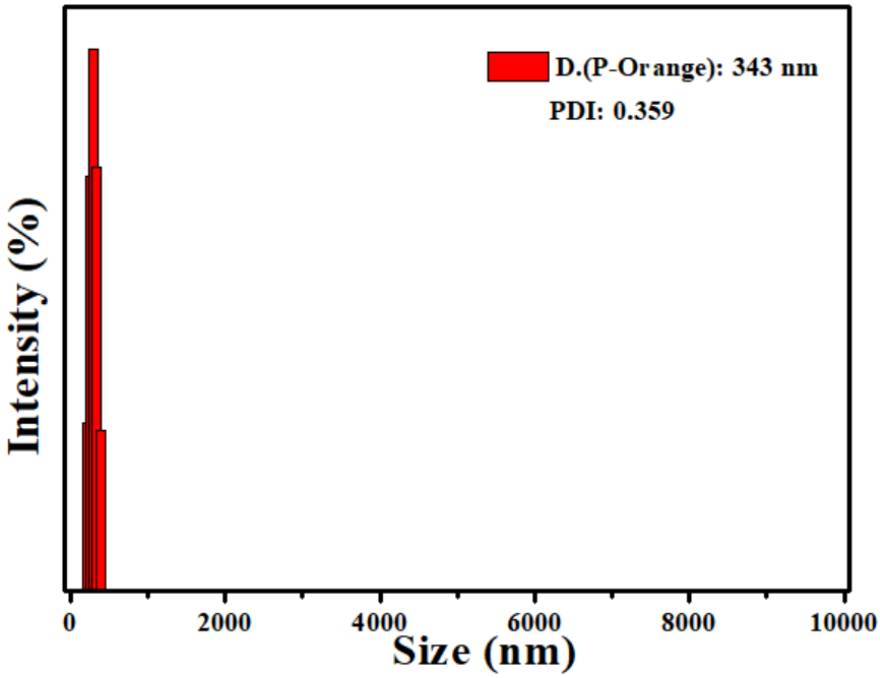

Fig. S25 The particle size distributions of P-Orange.

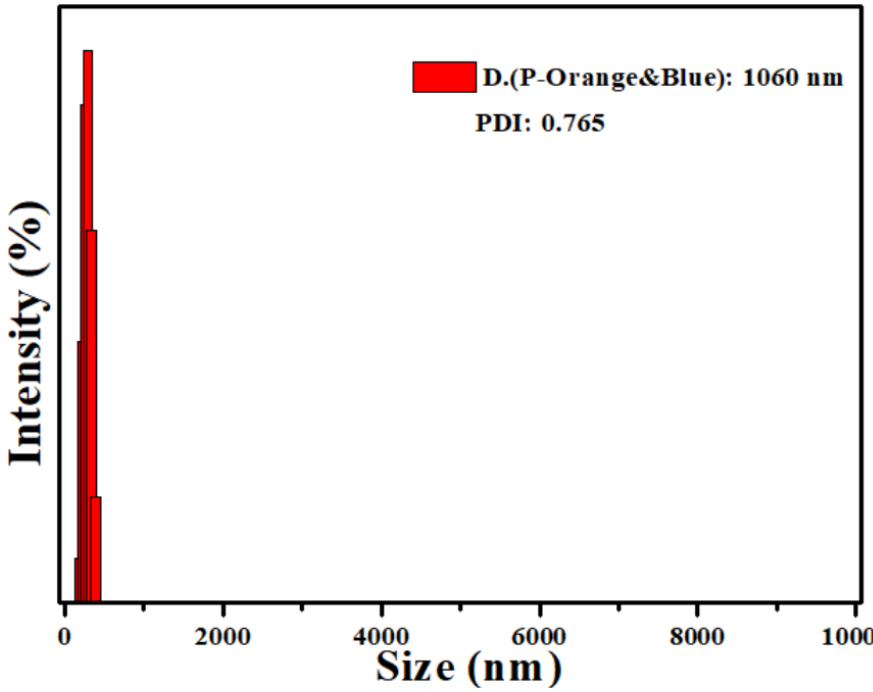

Fig. S26 The particle size distributions of P-Orange&Blue-3.

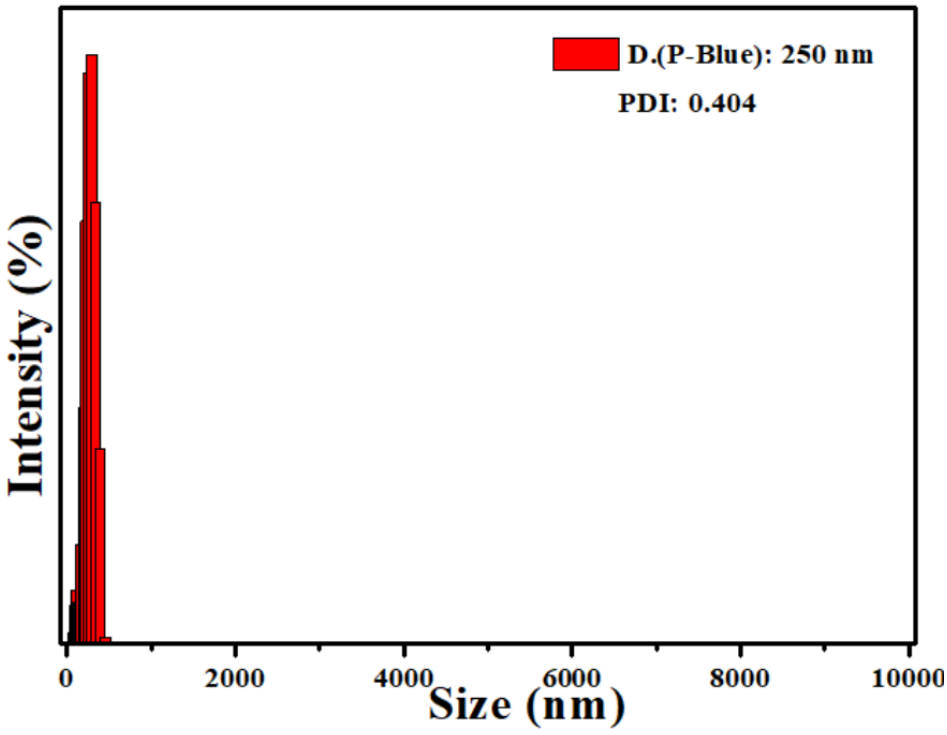

Fig. S27 The particle size distributions of P-Blue.

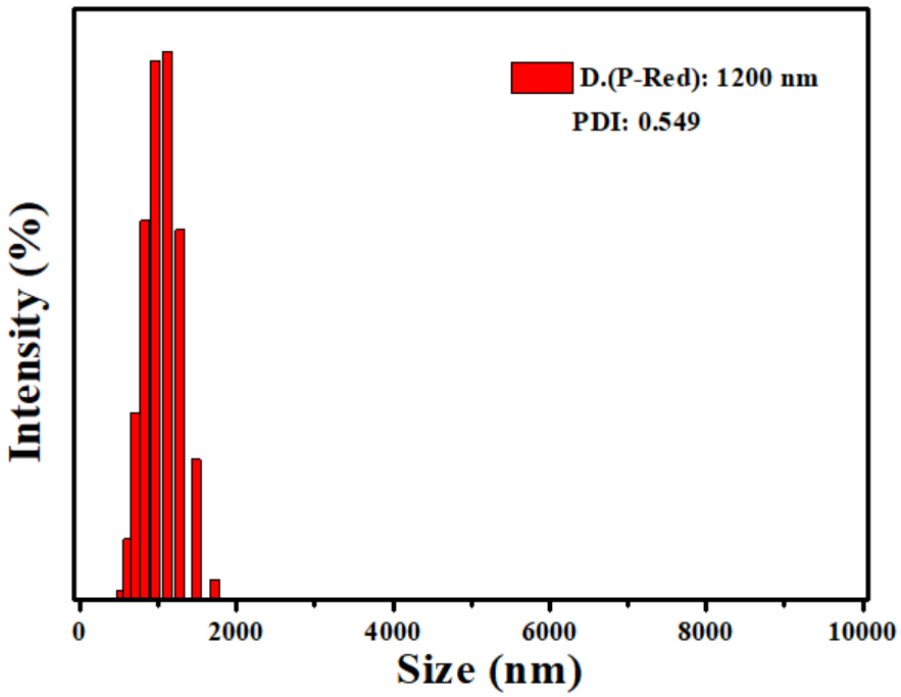

Fig. S28 The particle size distributions of P-Red.

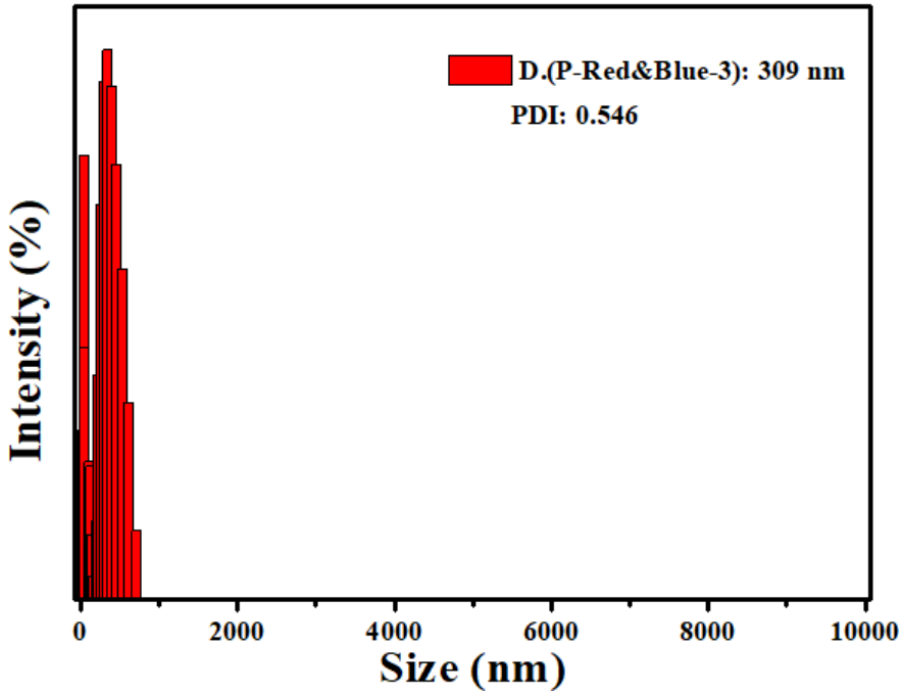

Fig. S29 The particle size distributions of P-Red&Blue-3.

20. The Fluorescence Spectra, photographs and SEM[7] images of hydrogels

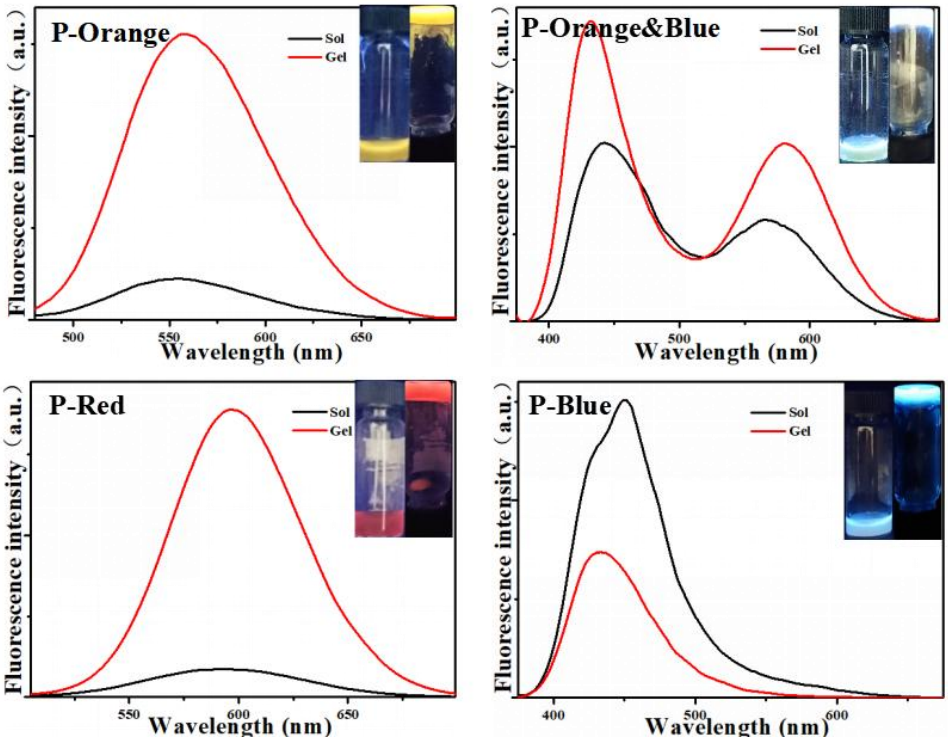

Fig. S30 The fluorescence spectra and photographs of P-Orange, P-Orange&Blue-3, P-Blue, P-Red in aqueous solution in the sol and gel states.

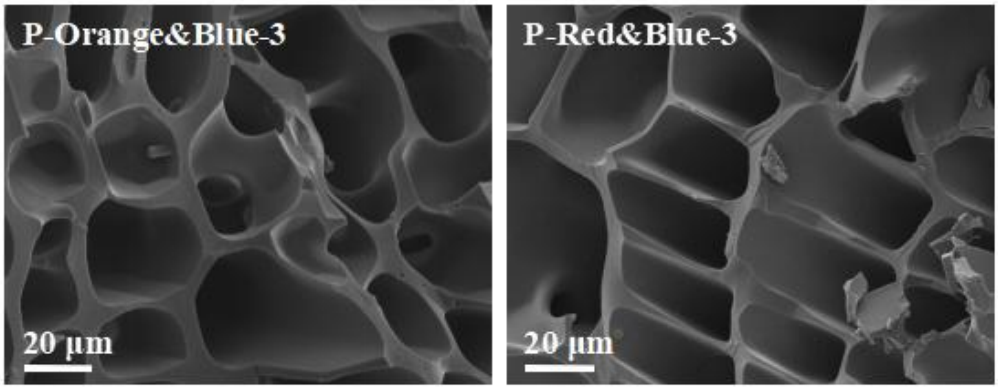

Fig. S31 SEM images of P-Orange&Blue-3 and P-Red&Blue-3 in the gel states.

[7] The morphology of xerogels of polymers were observed by scanning electron microscopy (SEM, Zeiss Ultra Plus), and the xerogel was produced by solvent evaporation by LGJ-10E multi-manifold freeze-drying machine. All of the samples were prepared according to the standard methods.

21. The UV and Fluorescence Spectra of P-Orange&Blue

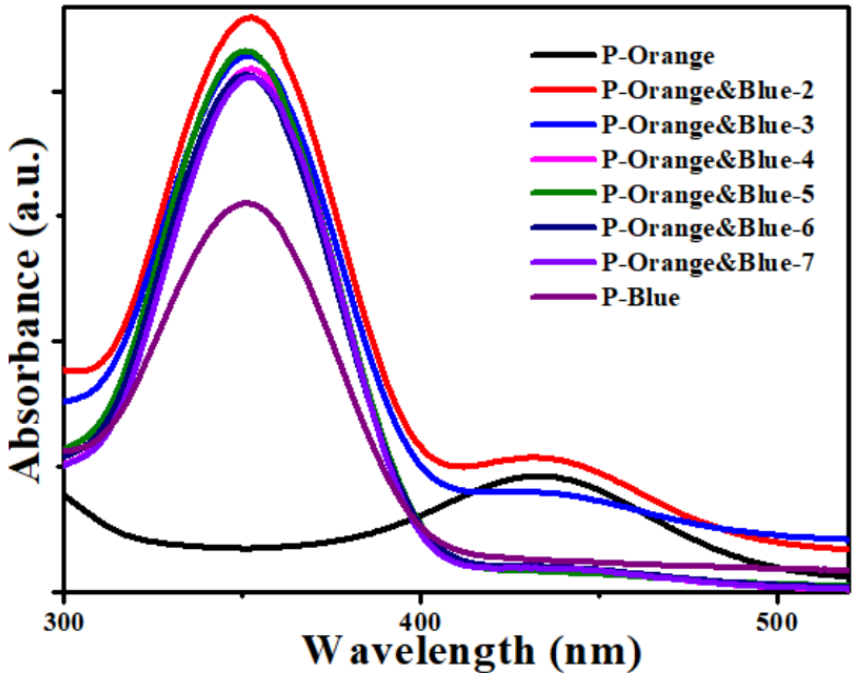

Fig. S32 The UV spectra of P-Orange&Blue in aqueous solution.

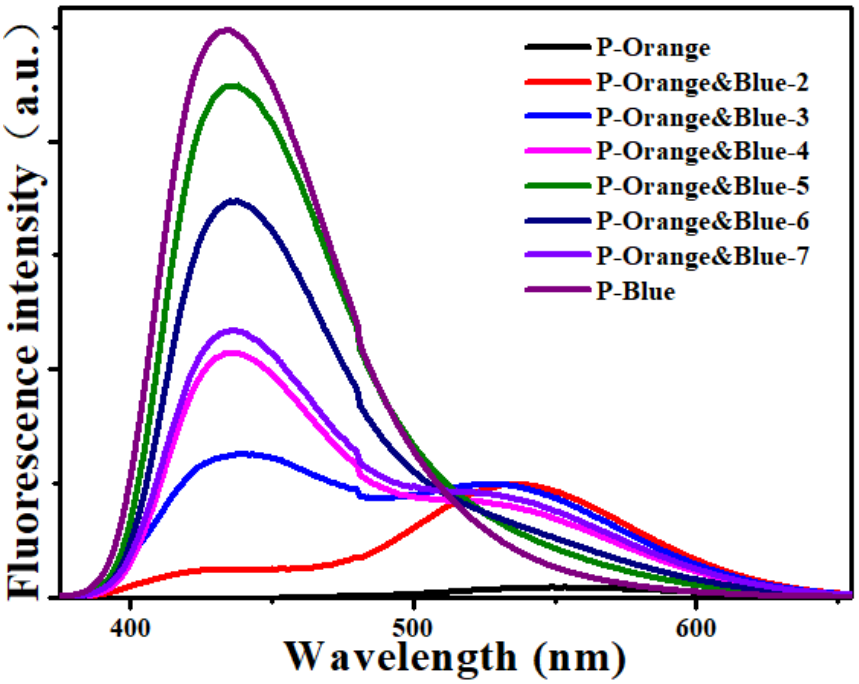

Fig. S33 The fluorescence spectra of P-Orange&Blue in aqueous solution.

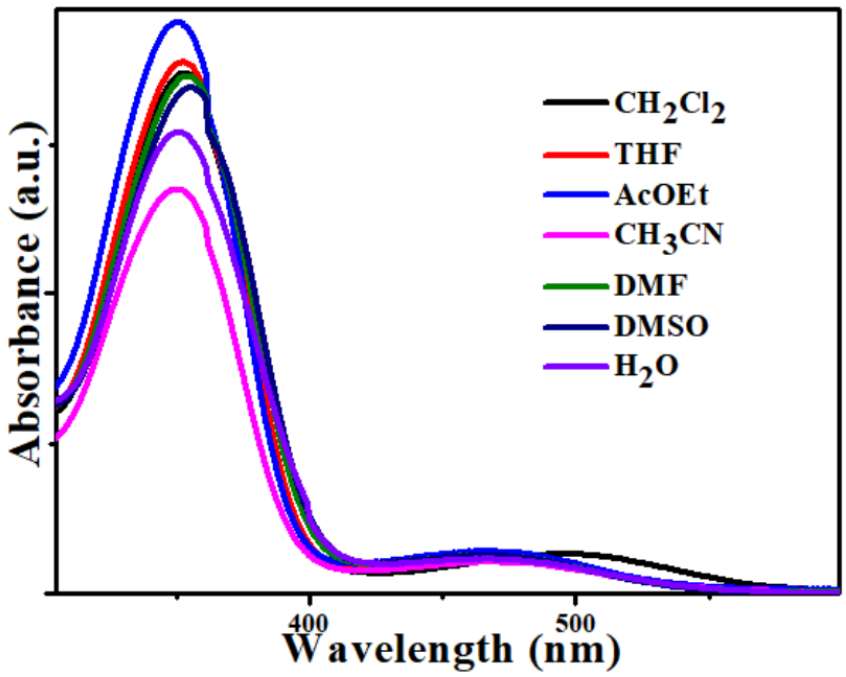

Fig. S34 The UV spectra of P-Orange&Blue-3 in different solution.

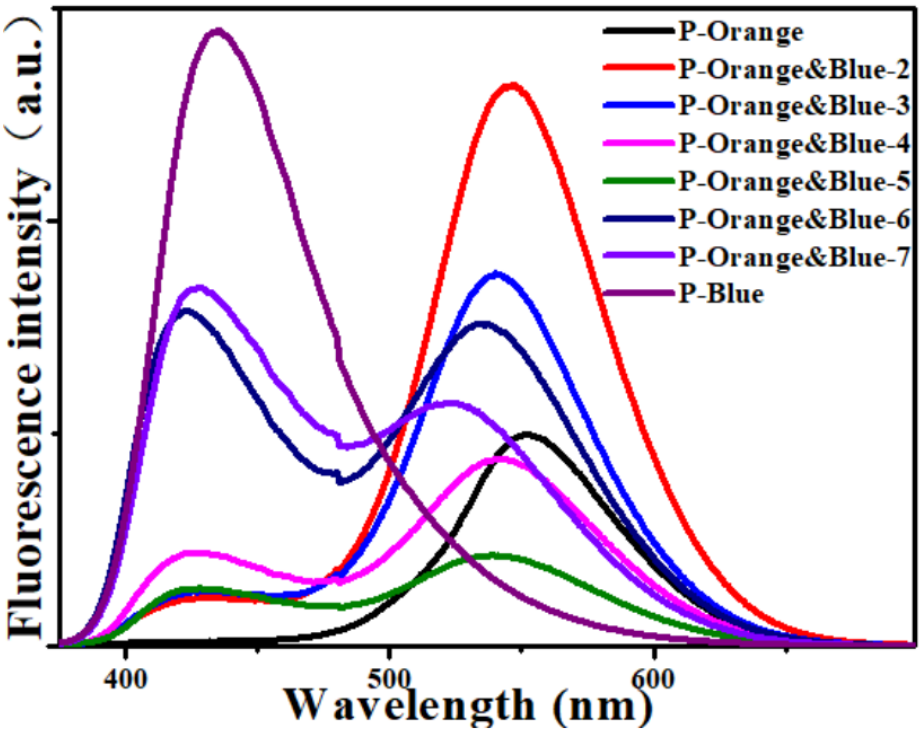

Fig. S35 The fluorescence spectra of P-Orange&Blue in solid state.

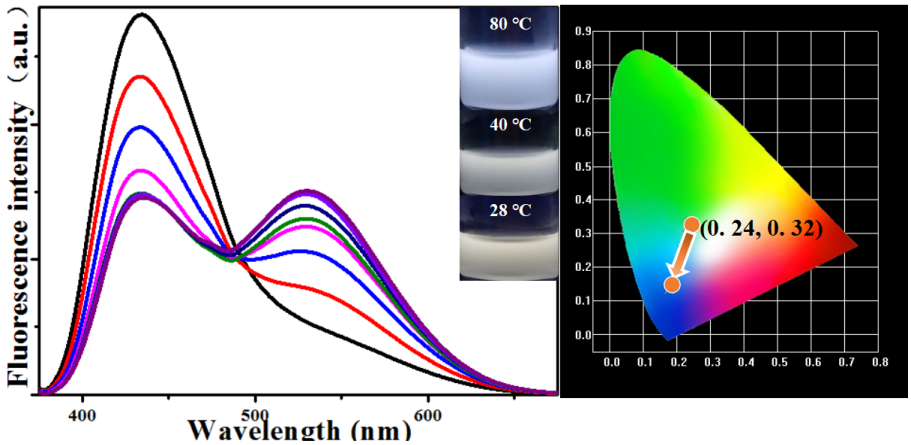

Fig. S36 The fluorescence spectra and photographs of P-Orange&Blue-3 in aqueous solution at different temperature under UV light (365 nm); The CIE Chromaticity Diagram of P-Orange&Blue-3 in aqueous solution at different temperature.

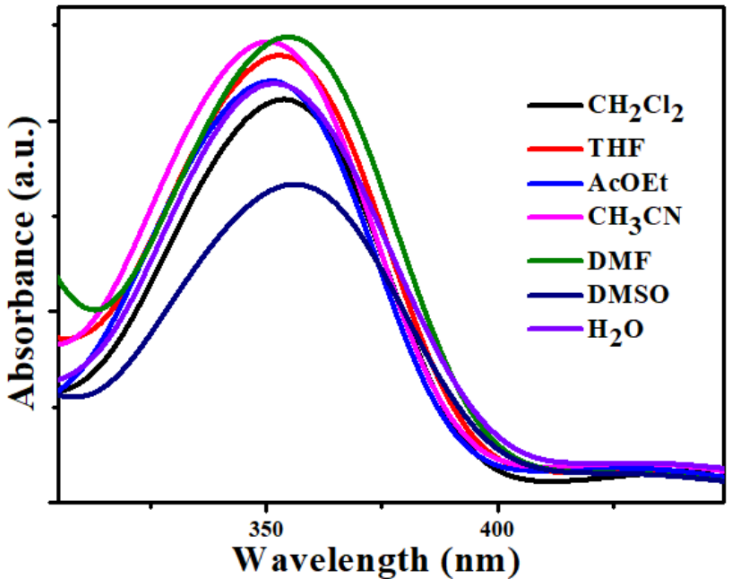

Fig. S37 The UV spectra of P-Red&Blue-3 in different solution.

22. **The UV and fluorescence spectra of P-Red&Blue**

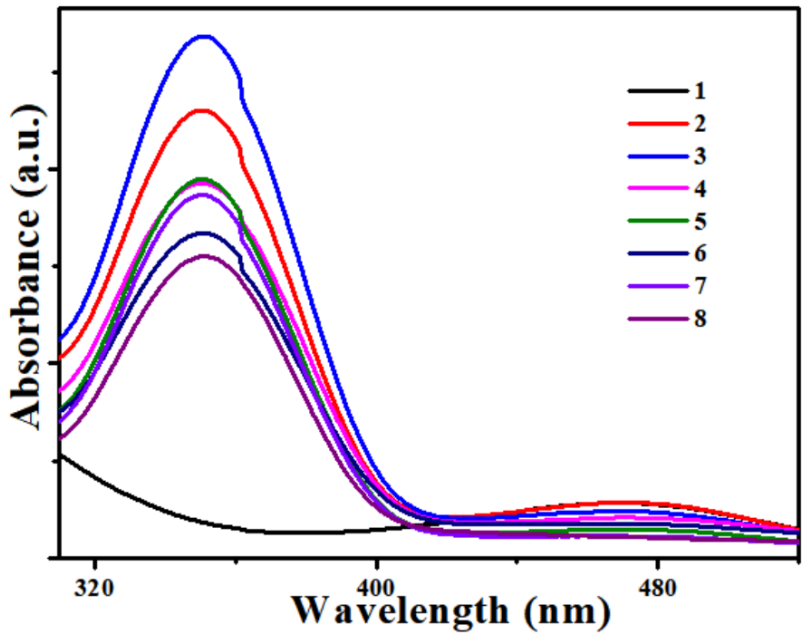

Fig. S38 The UV spectra of P-Red&Blue in aqueous solution.

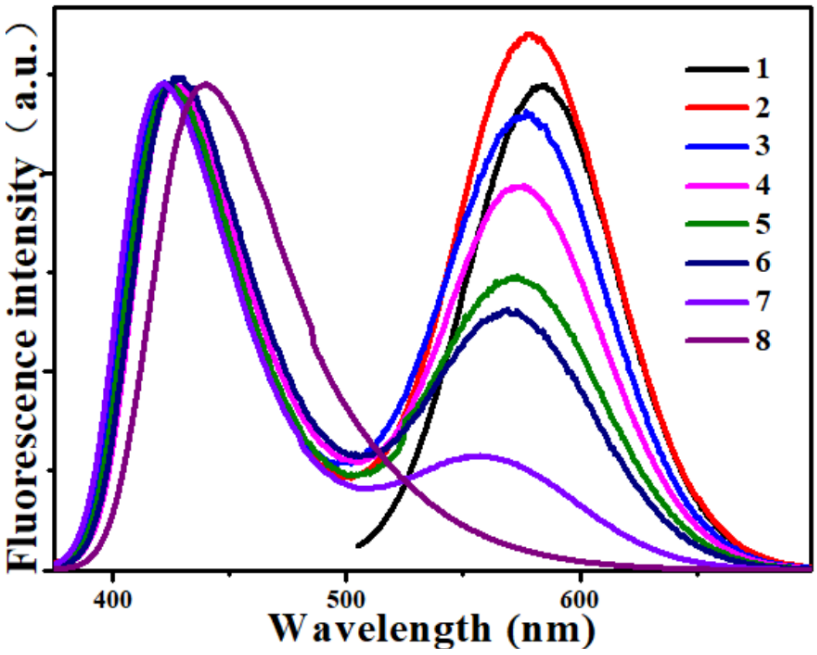

Fig. S39 The fluorescence spectra of P-Red&Blue in solid state.

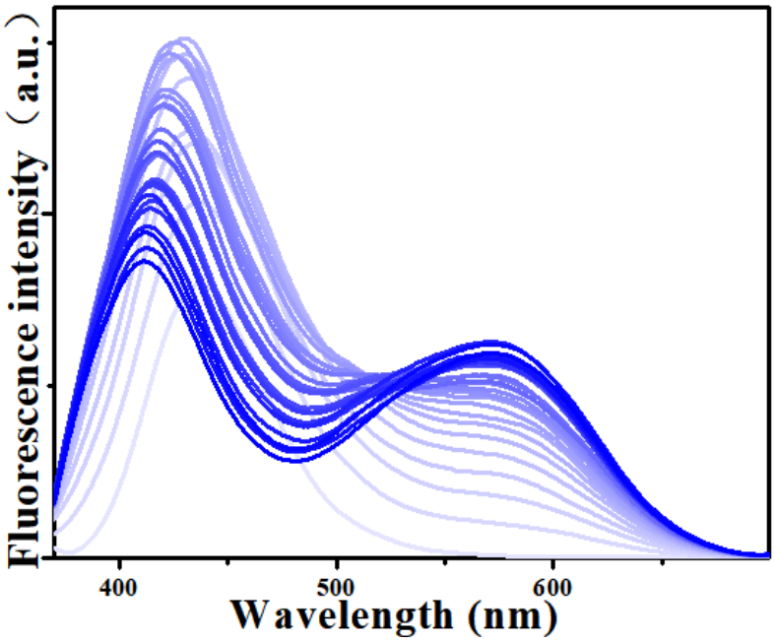

Fig. S40 The fluorescence spectra of different mass ratios of P-Red and P-Blue in ethyl acetate solution.

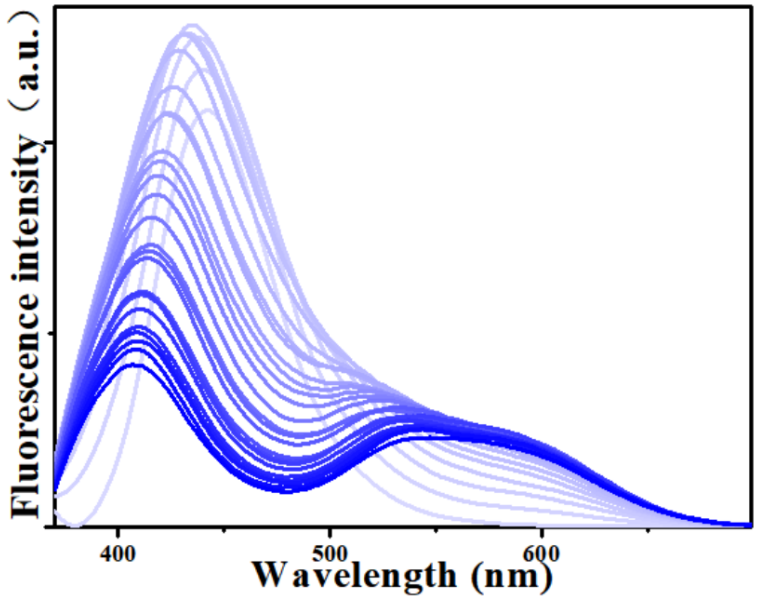

Fig. S41 The fluorescence spectra of different mass ratios of P-Red and P-Blue in THF solution.

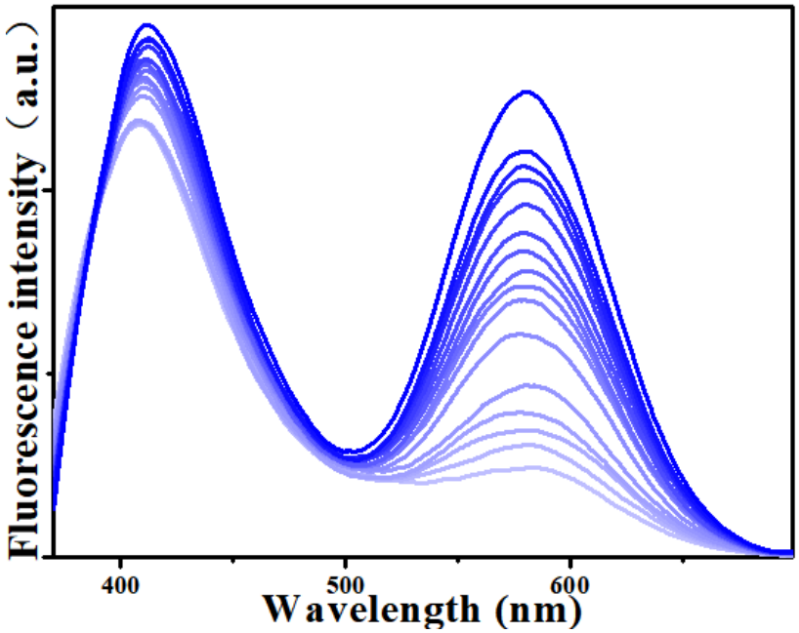

Fig. S42 The fluorescence spectra of different mass ratios of P-Red and P-Blue in aqueous solution.

23. The electrical conductivity of sodium chloride solution

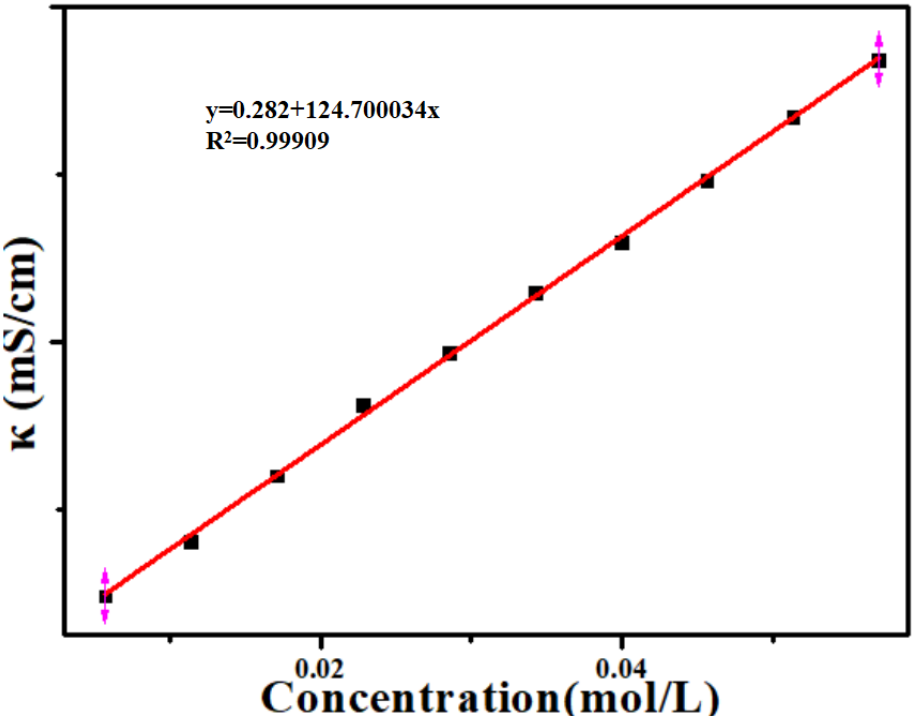

Fig. S43 The electrical conductivity of a linear fitting curve in sodium chloride solution at different concentrations.

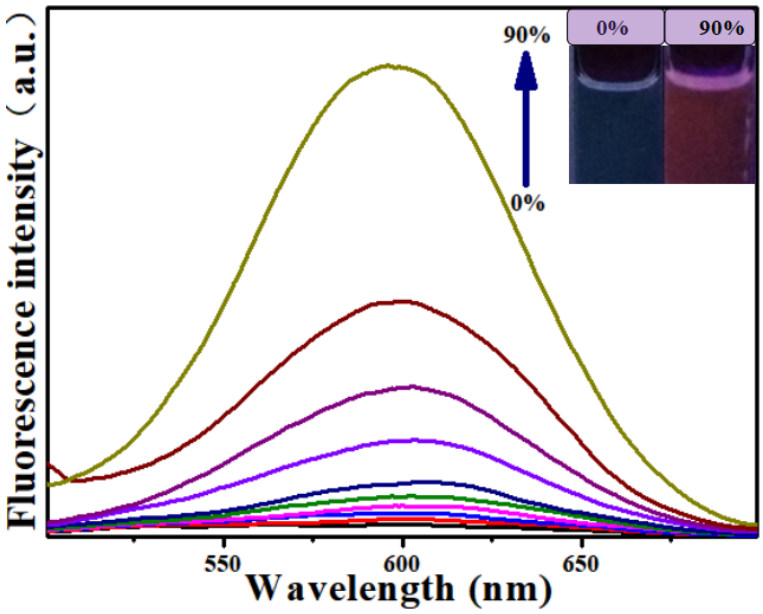

Fig. S44 The fluorescence spectra and photographs of TPA-Py-CVB with the $V_{glycerol}$: V_{MeOH} from 0 to 0.9.

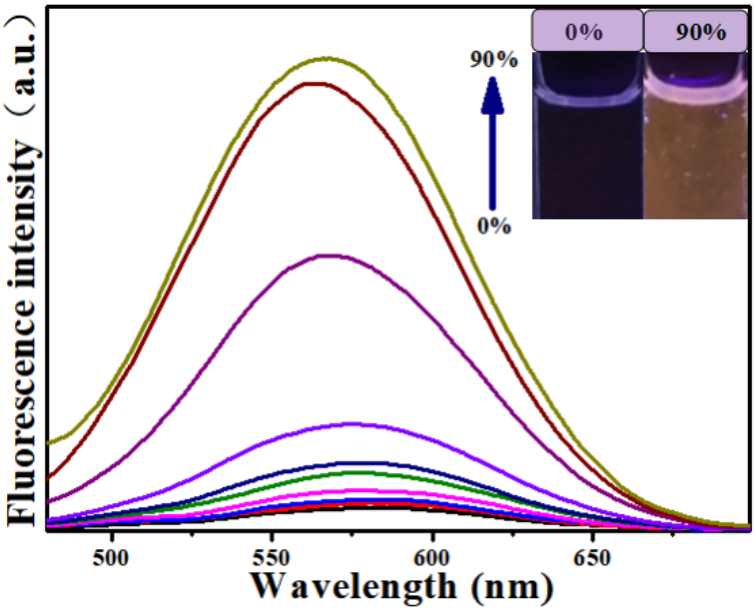

Fig. S45 The fluorescence spectra and photographs of TPA-VPy-CVB with the $V_{glycerol}$: V_{MeOH} from 0 to 0.9.

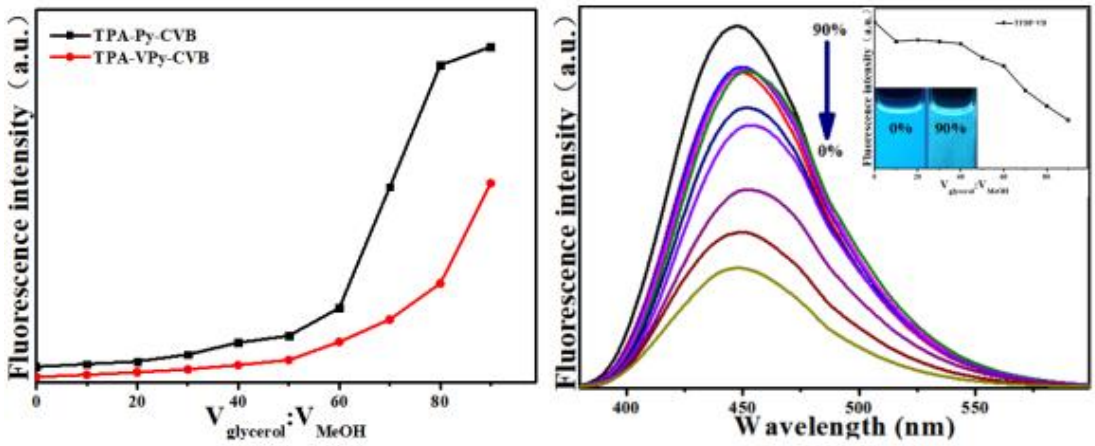

Fig. S46 Plots of maximum emission intensity of TPA-VPy-CVB and TPA-VPy-CVB with the $V_{glycerol}$: V_{MeOH} from 0 to 0.9. The Fluorescence Spectra and photographs of TFBP-VB with the $V_{glycerol}$: V_{MeOH} from 0 to 0.9.